Thermal Stabilities of the Microhydrated Zwitterionic Glycine: A Kinetics and Dynamics Study

Shan Xi Tian,* Xiang Sun,† Rui Cao, and Jinlong Yang

Hefei National Laboratory for Physical Sciences at Microscale, and Department of Chemical Physics, University of Science and Technology of China, Hefei, Anhui 230026, China

Received: July 18, 2008

Thermal stabilities of the zwitterionic glycine (zg) combined with water molecules are investigated by both ab initio/RRKM calculations and the thermostatic molecular dynamics (MD) simulations. The microhydrated zg clusters, zg-*n*w ($n = 2, 3$; w = water), can transfer to the canonical clusters cg-*n*w through the rapid intramolecular proton transfers (PT), while the proton is shifted via the intermolecular hydrogen bonds for zg-4w → cg-4w. Both the MD/solution model simulations and the RRKM calculations indicate that the zg and cg conformers hydrated with more water molecules have their respective higher stabilties and the transformation needs to overcome a certain energy barrier. The thermostatic MD simulations show that the dynamic PT processes are significantly influenced by both the temperatures used in the trajectory simulations and the hydrogen bonding arrangements between glycine and water molecules.

1. Introduction

Zwitterionic isomers of amino acids have been proved to be unstable in the gas phase while they exist in the condense phase.[1] However, they can be stabilized in the gas-phase clusters in which the zwitterions are solvated, e.g., with water molecules[2] or coordinated, e.g., with metal or molecular ions.[3] There are numerous theoretical[2a−c] and experimental studies[4] focusing on the elucidation of the stabilities of glycine-*n*w ($n = 1$ to several dozens, w means water molecule) complexes. There is a long-term argument about how many water molecules are necessary to stabilize the zwitterionic glycine (zg), indicating a strong dependence on the basis sets and the levels of theory used in the calculations.[2a] The experimental studies show that the zg can be stabilized at least by two water molecules,[4] which is supported by a recent theoretical work.[5] In these theoretical reports, the stable geometries corresponding to the local minima on the respective potential energy surfaces were obtained within the adiabatic approximation, namely, temperature $T \approx 0$ K. To date, there are no studies of the thermal dynamic stability of the zg-involved complex.

In this work, we report a theoretical study of the thermal stabilities of zg-*n*w ($n = 2, 3, 4$) clusters within both kinetics and dynamics schemes. The Rice-Ramsperger−Kassel−Marcus (RRKM)[6] formalism is used to measure the rate coefficients of the proton-transfer (PT) reactions between the zwitterionic and canonical isomers. Ab initio molecular dynamics (MD) simulations can mimic these fast PT processes. The thermostatic MD simulations at the different temperatures ($T = 298$, 598, and 898 K) show that the PT is strongly influenced by the environment temperatures and the hydrogen bonding (HB) arrangement around the ammonia group in the zg-*n*w clusters.

2. Computational Methods

The microhydrated zg-*n*w ($n = 2, 3, 4$) clusters shown in Figure 1 have been proved to be the most stable zwitterionic

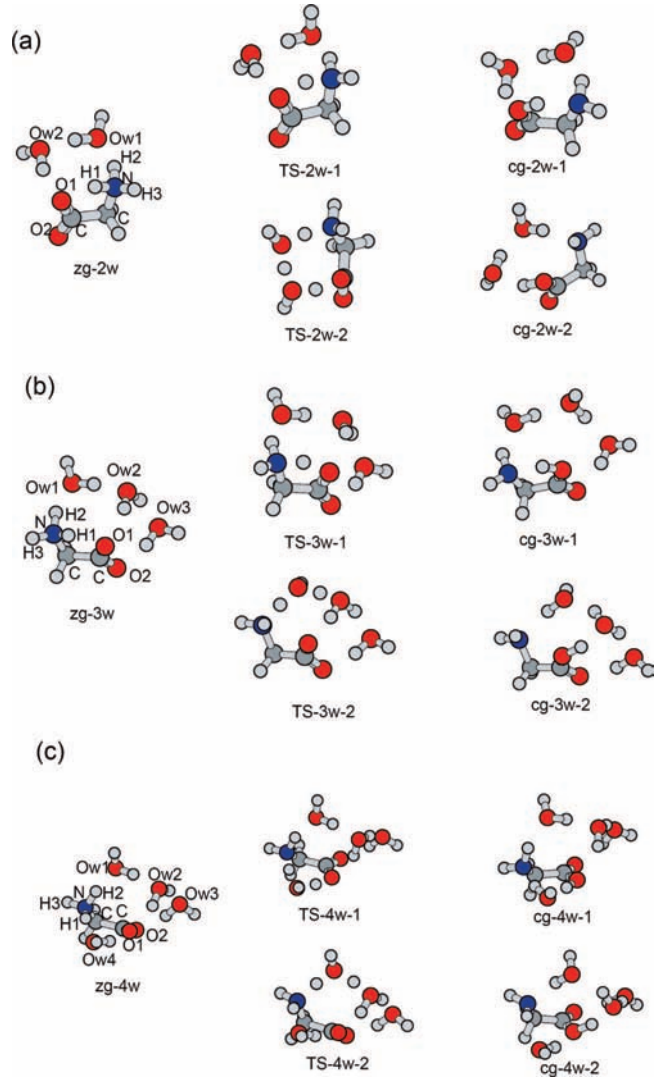

Figure 1. Optimized geometries of the zwitterionic glycine-*n* water ($n = 2, 3, 4$). The broken lines represent the hydrogen bonds.

* Corresponding author. E-mail: sxtian@ustc.edu.cn.
† Current address: Graduate student at the Department of Chemistry, Brown University, Providence, RI.

10.1021/jp8092594 CCC: $40.75
Published on Web 12/16/2008

TABLE 1: Relative Energies (kcal/mol) of Canonical and Zwitterionic Glycine−Water Clusters and Their Proton-Transfer Transition States

		zg-*n*w	TS-*n*w-1	TS-*n*w-2	cg-*n*w-1	cg-*n*w-2
$n = 2$	B3LYP/6-31G(d)	0.00	−1.26(1.31[b])	5.71	−6.17	−6.95
	B3LYP/6-31++G(d,p)	0.00	−1.42(0.41[b])	5.18	−6.81	−6.12
	MP4(SDTQ)[a]	0.00	−1.03(0.80[b])	8.88	−7.48	−7.37
$n = 3$	B3LYP/6-31G(d)	0.00	−0.28(3.03[b])	2.26	−2.15	−3.51
	B3LYP/6-31++G(d,p)	0.00	−1.04(1.45[b])	2.87	−5.06	−4.46
	MP4(SDTQ)[a]	0.00	−0.45(2.04[b])	6.04	−4.67	−4.76
$n = 4$	B3LYP/6−31G(d)	0.00	−4.46(1.45[b])	−3.82(7.84[b])	−1.33	−2.00
	B3LYP/6-31++G(d,p)	0.00	−3.03(6.98[b])	−3.97(7.89[b])	−0.24	0.42
	MP4(SDTQ)[a]	0.00	5.79	6.89	0.86	−0.40

[a] Over the B3LYP/6-31++G(d,p) optimized geometries. [b] Excluding the zero-point vibrational energy corrections.

species although they were less stableby 11.37, 8.40, and 6.04 kcal/mol in energy than the global minima canonical glycine clusters, cg-*n*w ($n = 2, 3, 4$), respectively.[5] Here they were reoptimized at the hybrid density functional B3LYP[7] level of theory together with 6-31G(d) and 6-31++G(d,p) basis sets. From zg-*n*w to cg-*n*w clusters, there were two possible PT routes, i.e., a direct intramolecular process and along the HB chain formed with water molecules. The corresponding transition states (TS-*n*w-1,2) and cg-*n*w-1,2 complexes were searched and their characters on the potential energy surfaces were confirmed at the B3LYP/6-31G(d) and B3LYP/6-31++G(d,p) levels. The MP4(SDTQ)[8] method was employed to calculate the relative energies over the B3LYP/6-31++G(d,p) optimized geometries. Using the results of the aforementioned calculations, carried out with the Gaussian 03 program,[9] the rate coefficients for the transitions between the zg-*n*w and cg-*n*w complexes were calculated by the RRKM method over a grid of energies up to 100 kcal/mol of internal energy. No tunneling correction was included because (1) in the most cases the rates are extremely high when the internal energy is above the reaction threshold and (2) the accuracy of a few kcal/mol for the barrier height does not warrant the attempt to achieve the accuracy addressed by a tunneling correction.

To mimic the fast PT processes, the MD simulations in which the atom-centered density matrix propagation (ADMP)[10] MD method combined with the B3LYP/6-31G(d) quantum chemistry calculations were applied. In the ADMP approach, an extended Lagrangian is used to propagate the density matrix on a basis of atom centered Gaussian functions. In the thermostatic MD, the kinetic energy of the system is kept constant by scaling the kinetic energy at each step. The thermostatic MD simulations at $T = 298$, 598, and 898 K were performed with a time step of 0.2 fs (the total time was 1000 fs) and the fictitious electronic mass of 0.1 amu bohr.[2] For comparison with the above microhydrated glycine clusters, the polarized continuum model (PCM)[11] was used to produce the aqueous environment. The single zg tautomer combined with the PCM was first optimized at the B3LYP/6-31G(d) level, then it was propagated at the different temperatures. To avoid the computational collapse, the united atom topological model was replaced with Bondi's atom radii in the construction of the solute cavity.[11c]

3. Results and Discussion

The structures of glycine-*n*w ($n = 2$, 3, and 4) clusters and the transition states whose geometrical parameters are optimized at the B3LYP/6-31++G(d,p) level are depicted in Figure 1. There are no distinct structural differences between the B3LYP/6-31G(d) and B3LYP/6-31++G(d,p) results (the structural information is given as the Supporting Information). The relative energies respective to zg-*n*w are listed in Table 1. The B3LYP

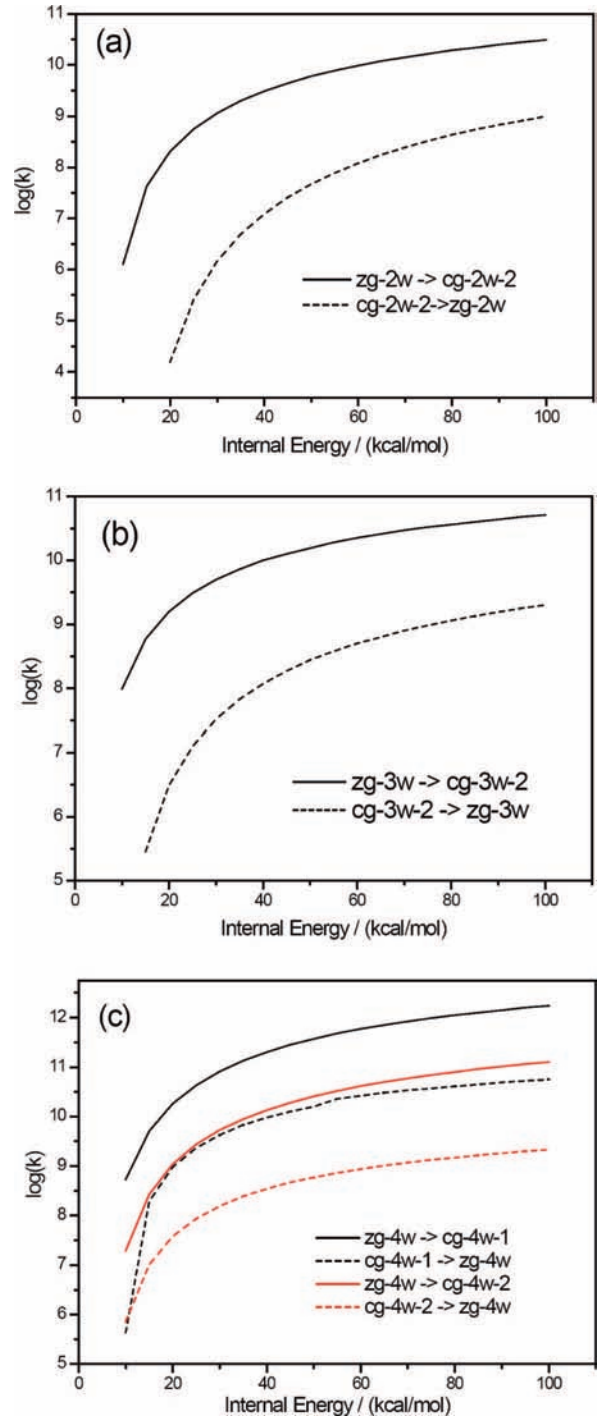

Figure 2. RRKM rate constants of the proton-transfer reactions between the zwitterionic and canonical isomers.

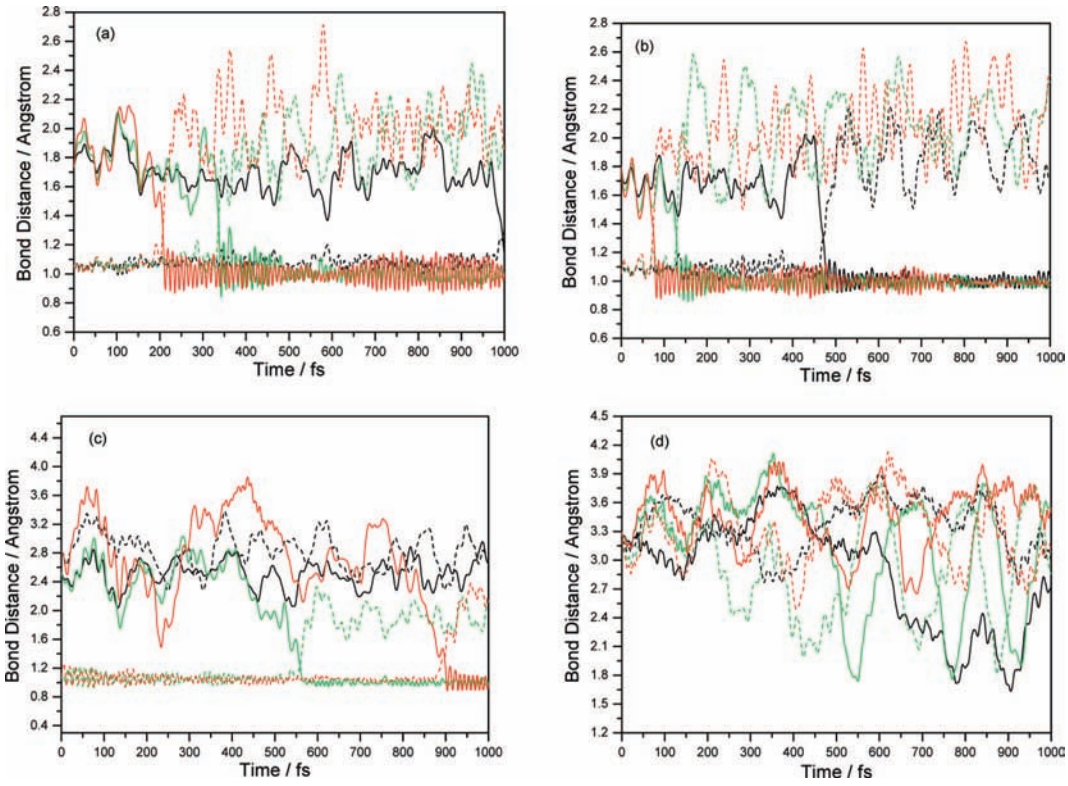

Figure 3. Bond distance changes at $T = 298$ (black), 598 (green), and 898 K (red). In panels a (zg-2w) and b (zg-3w), the solid lines represent O1···H1 and the broken lines represent N−H1. In panel c (zg-4w), the black ($T = 298$ K) solid and broken lines represent O_{w4}···H1 and O_{w2}···H2 distances, respectively, the green ($T = 598$ K) solid and broken lines represent O1···H1 and N−H1 distances, respectively, and the red ($T = 898$ K) solid and broken lines represent O1···H2 and N−H2 distances, respectively. In panel d (zg-PCM), the solid and broken lines represent O1···H1 and O1···H2 distances, respectively.

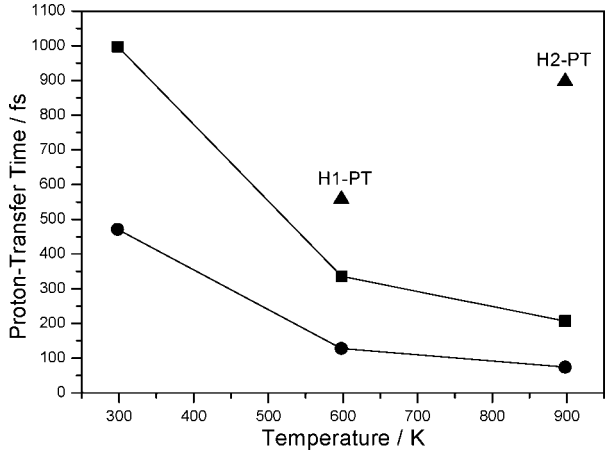

Figure 4. Comparison of the proton-transfer time: (■) zg-2w; (●) zg-3w, and (▲) zg-4w.

calculations predict the extremely low energy barriers for the zg-*n*w → cg-*n*w-1 ($n = 2, 3$) transitions. When the zero-point vibrational energy (ZPVE) corrections of the transition states TS-*n*w-1 are considered, these transitions become barrier-free. This indicates that the intramolecular zg → cg PT processes are energetically favorable.

In the zg-4w cluster, two hydrogen atoms (H1 and H2) are hydrogen bonded with two water molecules, w1 and w4, respectively. Thus, two intermolecular PT processes should be competitive. The energy barriers for zg-4w → cg-4w-1 and zg-4w → cg-4w-2 are comparable. The extrapolated MP4(SDTQ)/6-31++G(d,p) calculations predict the low energy barriers, 5.79 and 6.89 kcal/mol, for the above transitions, but they provide the qualitatively same results as the B3LYP calculations for zg-*n*w → cg-*n*w-1,2 ($n = 2, 3$).

One also can find that when the zg conformer is hydrated with two or three water molecules, the zg-*n*w clusters are still higher in energy than the cg-*n*w clusters, although these cg-*n*w clusters are not the most stable ones on the potential energy surfaces.[5] When the zg conformer is hydrated with four water molecules, the zg-4w and cg-4w clusters are comparable in energy, implying that the hydration with more water molecules ($n > 4$) will enhance the stability of zg.

Due to the fact that the B3LYP usually underestimates the barrier energies, the energies predicted with MP4(SDTQ) are used in the RRKM calculations. The harmonic vibration frequencies and ZPVE values calculated with B3LYP/6-31++G(d,p) are still used in the RRKM calculations. The very fast intramolecular PT processes for zg-2w → cg-2w-1 and zg-3w → cg-3w-1 are not considered here because of their extremely low or even negative barrier energies. In Figure 2, the RRKM rate constants for zg-2w ↔ cg-2w-2, zg-3w ↔ cg-3w-2, zg-4w ↔ cg-4w-1, and zg-4w ↔ cg-4w-2 are plotted. In general, for the internal energy 60−100 kcal/mol, the transition rates to the canonical clusters are in order of zg-4w > zg-3w > zg-2w. In the zg-4w ↔ cg-4w transitions, the intermolecular PT via the HB chain N−H1···O_{w4}−H···O1 (i.e., TS-4w-1) is faster than that via N−H2···O_{w1}−H···O_{w2}−H···O2 (i.e., TS-4w-2). Their reverse transition rates are normally slower because of the higher barrier energies. Two competitive PT processes to form the zwitterions, cg-4w-1 → zg-4w and cg-4w-2 → zg-4w, also have distinctly different rates in the internal energy range of 20−100 kcal/mol.

It is noted that only higher internal energies are considered, but the tunneling PT is excluded in the above RRKM calcula-

tions. There is no information about how fast the intramolecular PT processes, e.g., zg-2w → cg-2w-1 and zg-3w → cg-3w-1, are. To elucidate these fast dynamic processes and their dependence on the internal energy (here it is temperature used in the thermostatic simulation), the on-the-fly thermostatic MD simulations are performed.

The PT processes in the transitions can be found in Figure 3. More details of the MD trajectories are given as Supporting Information. Here we pay more attention to the temperature dependence of the PT. In Figure 3a describing the zg-2w dynamic trajectories, one can find that the H1-atom PT from the NH_3 to C═O1 occurs at 997, 336, and 207 fs for $T = 298$, 598, and 898 K, respectively.[12] At the simulation end (i.e., time = 1000 fs) for $T = 298$ K, see the Supporting Information, the HB interaction between water and C═O1 is removed but a weak HB with C═O2 is formed. The HB rearrangement can also be observed in the $T = 598$ K simulation, namely, a water dimer is loosely connected with the canonical glycine via a weak HB OW1···N−H2. However, only one water molecule is hydrogen bonded with the COOH group, while the other water molecule is vaporized at $T = 898$ K.

For the zg-3w cluster, see Figure 3b, the H1-atom PT from the NH_3 to C═O1 occurs at 471, 128, and 74 fs for $T = 298$, 598, and 898 K, respectively. When time is 1000 fs, the HB interaction O_{W2}−H···O1 vanishes upon the PT and a ten-atom HB chain N···H1−O1···H−O_{W3}···H1−O_{W2}···H−O_{W1}···H−N is formed for the $T = 298$ K simulation. It is interesting that three water molecules are detached completely at $T = 598$ K, and finally, a water trimer is formed with the more than 6 Å distance from the canonical glycine. At $T = 898$ K, all water molecules are vaporized and disjunctive. The farthest water molecule is about 14 Å from the canonical glycine.

In contrast to the above two clusters, for the zg-4w cluster (see Figure 3c), at $T = 298$ K, there are no PT processes. The H1 atom is transferred at 558 fs for the $T = 598$ K simulation and the H2 atom is transferred at 897 fs for the $T = 898$ K simulation. These PT differences may be interpreted by the two-side HB interactions, O_{W1}···H2−N and O_{W4}···H1−N, around the ammonia group in the zg-4w cluster; furthermore, these two HB interactions obstruct the formation of the intramolecular HB O1···H−N. However, there are the one-side water HB chains in the zg-2w and zg-3w clusters and the intramolecular HB O1···H−N. When time is 1000 fs, a butterfly-like water tetramer is about 3 Å from the canonical glycine at $T = 598$ K, while one water molecule is loosely combined with the canonical glycine and the other three water molecules form a chain-like cluster at $T = 898$ K.

The Bondi's atom radii used in the solution dynamic simulations permit the chemical bond formation and cleavage in the simulations, but the present APMD/PCM simulations do not show any PT processes. As shown in Figure 3d, the distances between O1 and H1 or H2 atoms vary dramatically, which means the rotations of the ammonia group on the N−C bond axis. This is also in line with the above energetic calculations, namely, the stability of zg can be enhanced by more solvated water molecules.

4. Conclusion

The present ab initio/RRKM calculations predict the stabilities of the microhydrated glycine clusters and the transition rate constants for zg-*n*w ↔ cg-*n*w ($n = 2$, 3, and 4). The very fast PT processes to the canonical clusters for the microhydrated zg-*n*w are further investigated by cooking at different temperatures in the thermostatic MD simulations, in which the PT processes for zg-2w and zg-3w prefer the direct intramolecular processes, and the faster PT occurs at the higher temperature. As clearly shown in Figure 4, for the zg-4w cluster, the intermolecular PT processes of the H1 and H2 atoms via the HB chain can be competitive. At the higher temperatures, the glycine molecule is intact while the solvent molecules are vaporized. In our previous work, the intramolecular PT of the β-alanine cation is almost unaffected by the environment temperatures.[13] However, the aqueous solvent effect on the PT time is observed by using the microhydration model in this work. This will be a great helpful toward understanding the properties of the zwitterionic amino acids.

Acknowledgment. This work is supported by NSFC (Grant No. 20673105), MOST National Basic Research Program (Grant No. 2006CB922004), and 973 Program (Grant No. 2007CB815204). S.X.T. gratefully acknowledges the support from the NCET program of the Ministry of Education of China.

Supporting Information Available: The coordinates of clusters predicted at the B3LYP/6-31++G(d,p) level, the other bond distance variances in the MD simulations, and the conformational changes of the clusters. This material is available free of charge via the Internet at http://pubs.acs.org.

References and Notes

(1) (a) Godfrey, P. D.; Brown, R. D. *J. Am. Chem. Soc.* **1995**, *117*, 2019. (b) Ding, Y.; Krogh-Jespersen, K. *Chem. Phys. Lett.* **1992**, *199*, 261. (c) Csaszar, A. G. *J. Am. Chem. Soc.* **1992**, *114*, 9568.

(2) For examples see: (a) Jensen, J. H.; Gordon, M. S. *J. Am. Chem. Soc.* **1995**, *117*, 8159. (b) Wang, W.; Pu, X.; Zheng, W.; Wong, N.-B.; Tian, A. *J. Mol. Struct. (THEOCHEM)* **2003**, *626*, 127. (c) Chaudhari, A.; Sahu, P. K.; Lee, S.-L. *J. Chem. Phys.* **2004**, *120*, 170. (d) Bolm, M. N.; Compagnon, I.; Polfer, N. C.; von Heldn, G.; Meijer, G.; Suhai, S.; Paizs, B.; Oomens, J. *J. Phys. Chem. A* **2007**, *111*, 7309.

(3) For examples see: (a) Bush, M. F.; Oomens, J.; Saykally, R. J.; Williams, E. R. *J. Am. Chem. Soc.* **2008**, *130*, 6463. (b) Wu, R.; McMahon, T. B. *J. Am. Chem. Soc.* **2008**, *130*, 3065. (c) Wu, R.; McMahon, T. B. *Angew. Chem., Int. Ed.* **2007**, *46*, 3668.

(4) Alonso, J. L.; Concinero, E. J.; Lesarri, A.; Sanz, M. E.; Lopez, J. C. *Angew. Chem., Int. Ed.* **2006**, *45*, 3471.

(5) Bachrach, S. M. *J. Phys. Chem. A* **2008**, *112*, 3722.

(6) (a) Holbrook, K. A.; Pilling, M. J.; Robertson, S. H. *Unimolecular Reactions*; Wiley: Chichester, UK, 1996. (b) Forst, W. *Theory of Unimolecular Reactions*; Academic Press: New York, 1973.

(7) (a) Becke, A. D. *J. Chem. Phys.* **1993**, *98*, 5648. (b) Lee, C.; Yang, W.; Parr, R. G. *Phys. Rev. B* **1988**, *37*, 785.

(8) Krishnan, R.; Pople, J. A. *Int. J. Quantum Chem.* **1978**, *14*, 91.

(9) Frisch, M. J.; et al. *Gaussian 03*; Gaussian, Inc.: Pittsburgh, PA, 2003.

(10) (a) Schlegel, H. B.; Millam, J. M.; Iyengar, S. S.; Voth, G. A.; Daniels, A. D.; Scuseria, G. E.; Frisch, M. J. *J. Chem. Phys.* **2001**, *114*, 9758. (b) Iyengar, S. S.; Schlegel, H. B.; Millam, J. M.; Voth, G. A.; Scuseria, G. E.; Frisch, M. J. *J. Chem. Phys.* **2001**, *115*, 10291. (c) Schlegel, H. B.; Iyengar, S. S.; Li, X.; Millam, J. M.; Voth, G. A.; Scuseria, G. E.; Frisch, M. J. *J. Chem. Phys.* **2002**, *117*, 8694.

(11) (a) Cances, M. T.; Mennucci, V.; Tomasi, J. *J. Chem. Phys.* **1997**, *107*, 3032. (b) Barone, V.; Cossi, M.; Tomasi, J. *J. Comput. Chem.* **1998**, *19*, 404. (c) Barone, V.; Cossi, M.; Tomasi, J. *J. Chem. Phys.* **1997**, *107*, 3210.

(12) The proton transfer time is defined as the time when the H atom is just at the middle point between two atoms or along the transferring path.

(13) Tian, S. X.; Yang, J. *J. Chem. Phys.* **2007**, *126*, 141103.

JP8092594